Jurnal Polimesin
Department of Mechanical Engineering
State Polytechnic of Lhokseumawe
http://e-jurnal.pnl.ac.id/polimesin

e-ISSN : 2549-1999 No. : 3 Month : June
p-ISSN : 1693-5462 Volume : 21 Year : 2023

Article Processing Dates: Received on 2023-03-28, Reviewed on 2023-05-30, Revised on 2023-06-04, Accepted on 2023-06-06, and Available online on 2023-06-30

Simulation of turbulent non-premixed combustion in pulverized coal from Kalimantan Indonesia

A.P.Nuryadi*[1],Chairunnisa[1], Fitrianto[1], M.P. Helios[1],R.T. Soewono[1], R.J.Komara[2], I. Wulandari[3]

[1]Research Center for Energy Conversion and Conservation, National Research and Innovation Agency, National Research and Innovation Agency, South Tangerang 15314, Indonesia
[2]Directorate of Laboratory Management, Research Facilities, and Science and Technology Park, National Research and Innovation Agency, South Tangerang 15314, Indonesia
[3]Research Center for Hydrodynamics Technology, National Research and Innovation Agency, Surabaya 60112, Indonesia
*Corresponding author: agus130@brin.go.id

Abstract
A computational simulation was created to investigate pollutants during coal combustion in a Drop Tube Furnace using Kalimantan coal. Previous research has explored Drop Tube Furnace combustion with Kalimantan coal, but lacked an understanding of combustion phenomena and pollutants, which are challenging to observe experimentally. This study utilized three samples of Kalimantan coal, namely RP, MB, and KC, acquired from various mining sources. This research is new study of simulation combustion coal in Drop Tube Furnace using non-premixed turbulent combustion and the Probability Density Function model with structured grid. The study reports on the temperatures and mass fractions of pollutants, including NO_X, SO_2, and CO_2, along the centerline of the domain. The findings show that RP coal produced the highest combustion temperature, while KC coal produced the lowest. MB coal had the highest CO_2 mass fraction, KC coal had the highest NO_x value, and RP coal had the highest SO_2 value.

Keywords: Turbulent, Non-premixed, PDF, pollutant, Kalimantan Coals.

1 Introduction

Climate change and the depletion of the ozone layer have become worldwide concerns due to pollution [1]. Heavy metal emissions during combustion are linked to human diseases, environmental damage, and pollutants like CO_x, SO_x, and NO_x. The combustion process involves the reaction of nitrogen in the air with fossil fuels and oxygen, forming NO_x [2], [3]. The NO_x then reacts with ammonia and water vapor to form nitric acid and fine particles [4], [5]. Fossil fuels, primarily coal, are the primary source of electricity generation and contribute to CO_2 emissions [6]. One of the biggest coal producers in Indonesia, with approximately 900 million tons of coal reserves in Kalimantan, Indonesia needs 188.9 million tons of coal for power plants and industry in 2022 [7].

The Pulverized Coal boiler is widespread in Indonesia, whereby coal is crushed and dispersed into the combustion chamber. Generating energy through the compounding of pulverized coal is a prevalent method [8]. According to a study using Fluent, the Probability Density Function (PDF) was used to simulate coal pulverized combustion., which is more effective since fewer species transport equations must be solved [9]. The investigation also looked at how the distribution of gas and particles affected the radiant heat transmission in an axisymmetric pulverized coal combustion [10]. Another 2D model study was conducted to elucidate the impact of steam injection in reducing NO_x, CO, and C pollutants in pulverized coal burners [11]. In a two-dimensional chamber, pulverized coal was burnt under different conditions, specifically focusing on investigating the effects of injecting different gases, which aid in reducing pollutants. The researchers analyzed how these gases affected various parameters, such as temperature, velocity, and NO_x, at varying gas concentrations [12]. A model was created to investigate how NO_x is reduced while burning pulverized coal. The coal combustion was simulated using the SIMPLE method, and the interaction between turbulence and chemistry was simulated using the Probability Density Function (PDF) model [12].

Investigating the combustion of pulverized coal in cement plants involved numerical computations using Fluent. Applying the energy equation to estimate the internal flow field of temperature and the amounts of volatile chemicals and pollutants, which included both the traditional model (P1) and the non-premixed combustion model [13]. Investigation Two-dimensional combustion on blast furnace using Non-premixed coal particles are injected as a high-velocity stream, while air is supplied from the top and bottom inlets. Due to the symmetric geometry, only half of the domain was considered using Fluent [14]. The study of tangentially-fired pulverized coal boilers with PDF model and non-premix combustion depicts the condition of pulverized coal combustion, such as flame properties, coal burning patterns, and the release of NO_x pollutants [15]. Two-dimensional modelling pulverized combustion with three coal studied using steady-state turbulent non-premixed combustion. The impact of these different factors has been discussed upon peak temperature inside the furnace, heat transfer to/from the system to surroundings, and emission of gases using Fluent [16].

The combustion characteristics of coal were studied using a DTF, which aimed to replicate the conditions of coal-fired power plant boilers operating in supercritical or subcritical modes. The DTF experiment settings were determined by taking different operational factors into account. The DTF was operated at 1200 °C to describe a typical coal-fired power plant [17]–[20]. SEM-EDS and XRD analyses on Kalimantan coal support the result of the experiment on DTF [21].

Previous studies described burning coal using CFD, but each coal from each region has different characteristics and types of furnaces. This study conducted a 2D simulation of coal combustion from Kalimantan using three coal samples, including coal from South Kalimantan RP and coals from East Kalimantan KC and MB. The Probability Density Function (PDF) was employed to examine the combustion of pulverized coal under high temperatures. The geometry of the furnace and parameters were based on the Drop Tube Furnace (DTF) [21] as the CFD domain and boundary conditions. Fluent software was used to explain the phenomenon of combustion in the furnace and to compare the three samples of Kalimantan coal to identify the combustion characteristics and pollutants.

2 Research Methods

2.1 Mathematical models

Coal particles are dropped on the DTF header, and particles are assumed to be spherical and have a uniform diameter. The governing equations are Eq. 1-14 [9,22,23]:

- Continuity equation:

$$\frac{\partial \rho}{\partial t} + \nabla.(\rho\, \vec{u}) = 0 \quad (1)$$

- Momentum equation:

$$\frac{\partial}{\partial t}(\rho\vec{u}) + \nabla.(\rho\vec{u}\vec{u}) = -\nabla p + \nabla.(\bar{\bar{\tau}}) + \rho\vec{g} \quad (2)$$

- The energy equation:

$$\frac{\partial}{\partial t}(\rho H) + \nabla.(\rho\vec{u}H) = \nabla.\left(\frac{k_t}{C_p}\nabla H\right) + S_h \quad (3)$$

- H is the total enthalpy:

$$H = \sum_j Y_j H_j \quad (4)$$

S_h the origin of energy due to chemical reaction:

$$S_h = -\Sigma\frac{h_j^0}{M_j}R_j \quad (5)$$

- In this study, turbulent effects were considered by utilizing the ke-ε turbulent model [24]. The equation used to transport turbulent kinetic energy (K) is as follows:

$$\frac{\partial(\rho k)}{\partial t} + \nabla.(\rho\vec{u}k) = \nabla.\left[\left(\mu + \frac{\mu_t}{\sigma_k}\right)\nabla k\right] + G_k - \rho\varepsilon + P_K \quad (6)$$

- The model used for spectral intensity in radiation is the Discrete Ordinates (DO) model [25].

$$\nabla.(I_\lambda(\vec{r},\vec{s})\vec{s}) + (a_\lambda + \sigma_s)I_\lambda(\vec{r},\vec{s}) = a_\lambda n^2 I_{b\lambda} + \frac{\sigma_s}{4\pi}\int_0^{4\pi} I_\lambda(\vec{r},\vec{s}')\varphi(\vec{s},\vec{s}')d\Omega' \quad (7)$$

- Discrete Phase Model:

$$m_p\frac{d\vec{v}_p}{dt} = \Sigma\vec{F} \quad (8)$$

$\vec{F}$ is an external force. In this case, when dealing with small particles that have a high-density ratio, the dominant forces that affect the particle are drag and buoyancy forces. This leads to a specific equation of motion [26].

$$\frac{d\vec{v}_p}{dt} = F_D(\vec{v} - \vec{v}_p) + \frac{g(\rho_p - \rho)}{\rho_g} \quad (9)$$

- In this equation, R_{ep} is the particle Reynolds number, which is given as [27]:

$$Re_p = \left(\frac{\rho d_p|\vec{v}_p - \vec{v}|}{\mu}\right) \quad (10)$$

- As a function of particle Reynolds number is defined of drag coefficient (C_D), [28,29]:

$$C_D = \frac{24}{Re}(1 + 11.2355Re^{0.653}) + \frac{(-0.8271)Re}{8.8798 + Re} \quad (11)$$

- Coal devolatilization [20]:

$$\frac{-dm_p}{dt} = k(m_p - (1 - f_{v,0} - f_{w,0})m_{p,0}) \quad (12)$$

where:

$$K = A_1 exp^{\frac{-\varepsilon}{RT}}$$

- The Mixture Fraction and PDF [9], [30]:

Mean mixture fraction $(\bar{f})$:

$$\frac{\partial(\rho\bar{f})}{\partial t} + \nabla.(\rho\bar{f}\vec{u}) = \nabla.\left(\frac{\mu_t}{\sigma_t}\nabla\bar{f}\right) + \frac{\dot{m}_{p,0}}{m_{p,0}}(m_{p,in} - m_{p,out}) \quad (13)$$

Mean mixture fraction variance $(\bar{f}'^2)$:

$$\frac{\partial(\rho\bar{f}'^2)}{\partial t} + \nabla.(\rho\bar{f}'^2\vec{u}) = \nabla.\left(\frac{\mu_t}{\sigma_g}\nabla\bar{f}'^2\right) + 2.86\mu_t(\nabla\bar{f}'^2) - 2\rho\frac{\varepsilon}{k}\bar{f}'^2 \quad (14)$$

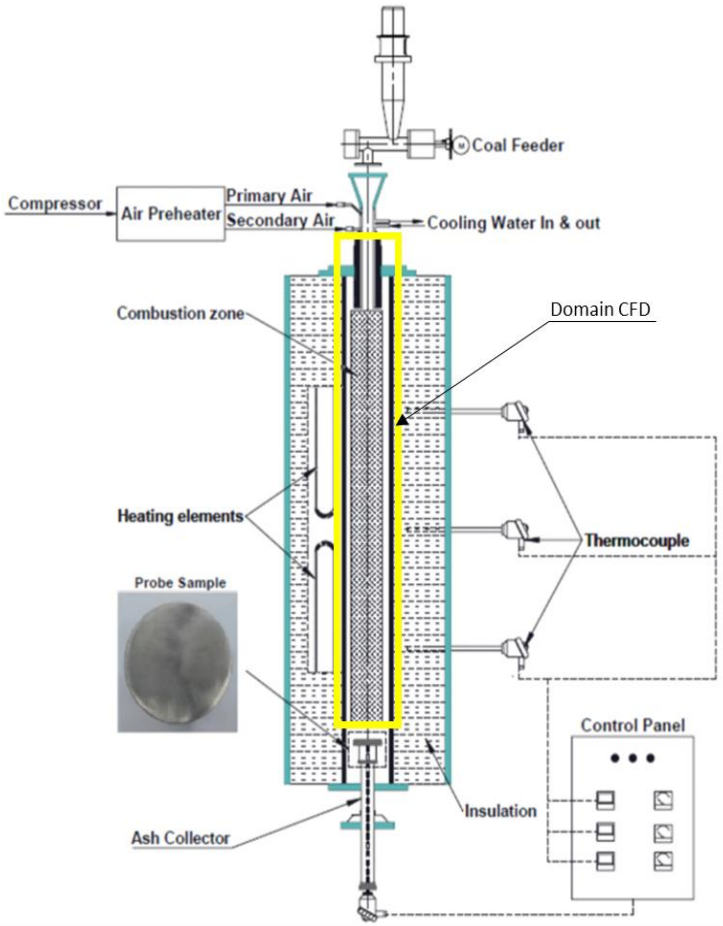

(a)

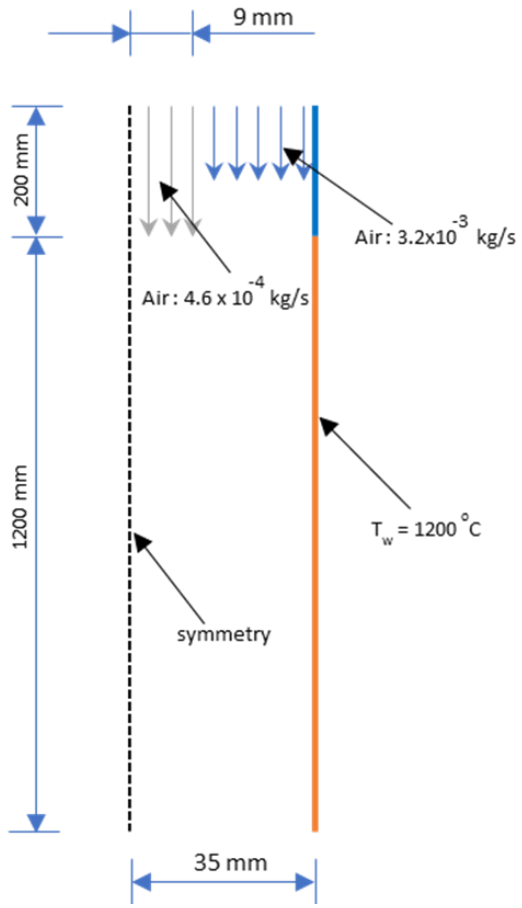

(b)

Fig. 1. (a) DTF schematic diagram DTF [21] and (b) CFD domain

Table 1. Kalimantan coals characteristics [21]

Proximate analysis	RP	KC	MB
Volatile Matter	43.28	39.7	40.04
Fixed carbon	38.16	44.08	44.47
Ash	6.78	6.88	3.2
Moisture	11.78	9.34	12.29
Ultimate Analysis			
C	59.48	66.24	59.64
H	4.08	4.43	4.42
O	28.72	20.48	31.59
N	0.75	1.37	1.03
S	0.19	0.6	0.12
Air			
N2	79	79	79
O2	21	21	21

Three coal samples from Kalimantan are analyzed proximally and ultimately in Table 1. Three main pathways can result in the formation of NOx during coal burning. The first is atmospheric nitrogen oxidation by the thermal NO process, followed by the Prompt NO mechanism, and the oxidation of nitrogen-containing fuels, including organic components, via the fuel-bound NO mechanism [31].

2.2 Numerical procedure

The DTF examines coal combustion properties with an alumina ceramic tube, 1200 mm in height and 35 mm in radius. 1 kWh electric heater with three zones can attain 1200 C heat in the furnace, and this setting was chosen to simulate a real-world pulverized coal boiler [21]. In the following phase of this research, the finite volume method with the residual weighting approach will be utilized to solve partial differential equations that regulate multispecies flows through FLUENT Software simulation.

The non-premix combustion model in Fluent has a coal calculator feature, which requires inputting the proximate and ultimate analysis data from Table 1. This model utilizes the Probability Density Function (PDF) to present the combustion products, namely CO_2 and SO_2 pollutants, as seen in this study. Additionally, the extended Zeldovich mechanism, a collection of temperature-dependent chemical events that control the synthesis of thermal NOx from molecular nitrogen, may be used in Fluent to search for NOx. This mechanism is a series of immediate reactions responsible for generating thermal NOx. [32].

$$O + N_2 \leftrightarrow N + NO$$
$$N + O_2 \leftrightarrow O + NO$$

At conditions close to stoichiometry and in mixtures rich in fuel, it has been observed that a third reaction plays a role in generating thermal NOx:

$$N + OH \leftrightarrow H + NO$$

A control volume is used, where each node corresponds to the computational domain so that the partial differential equations are integrated into each limited volume [33]. The QUICK is used for all convective terms, whereas the SIMPLE approach is applied to pressure/velocity terms [34]. The Probability Density Function (PDF) simulates the chemistry-turbulence interaction in a single transport equation. Additionally, a Discrete Phase Model (DPM) tracks the movement of 0.075-micron coal particles and analyzes their trajectory. Non-adiabatic heat transmission occurs when coal is burned to the mixture on the combustion chamber walls. The combustion chamber wall has a constant temperature of 1200°C, and an Air Fuel ratio of 1:7 is maintained. As a result, the isothermal boundary condition for the combustion chamber wall is established. To simplify the model, only half of the feeder and furnace chambers are simulated due to their symmetry, and the axes of symmetry are applied to the center line for the domain details shown in Fig. 1.

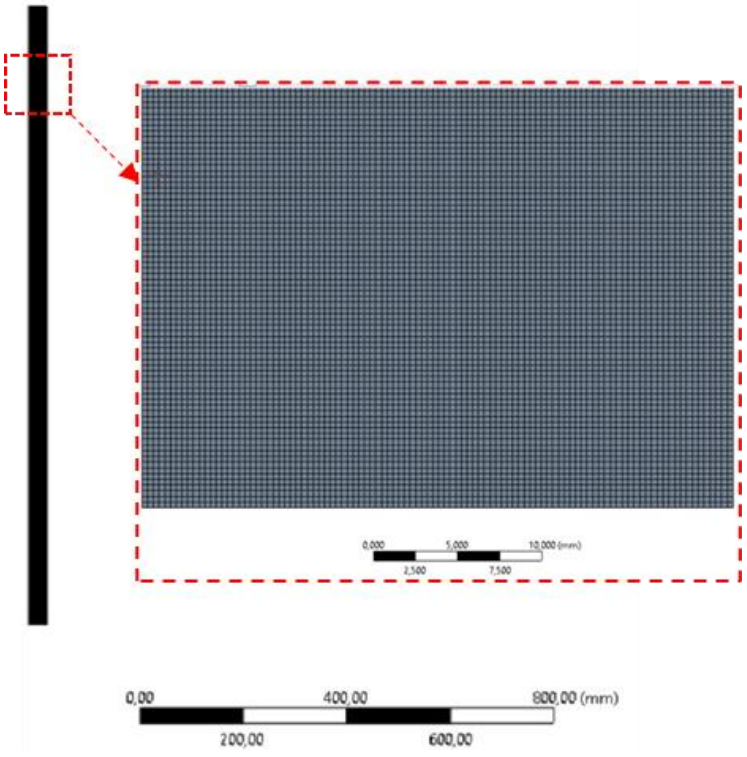

Fig. 2. Structured Grid

3. Results and Discussion.

A computational technique examines pollutants generated from pulverized coal combustion in a Drop Tube Furnace (DTF). Fig. 2 shows a structured grid in this study. The computational region is divided into sections using a structured grid. Five different grid distributions (Grid 1: 5036 nodes & 4900 elements, Grid 2: 102051 nodes & 100000 elements, Grid 3: 150772 nodes & 148230 elements, Grid 4: 200078 nodes & 197190 elements, Grid 5: 257823 nodes & 254560 elements) are tested to confirm that the computed outcomes are not influenced by the grid design. The results of the mass fraction of CO2 along the combustion chamber axis for the various grids are depicted in Fig. 3. The findings presented in the Fig. are used to conclude, Grid 3: 150772 nodes & 148230 elements were selected for all modeling cases.

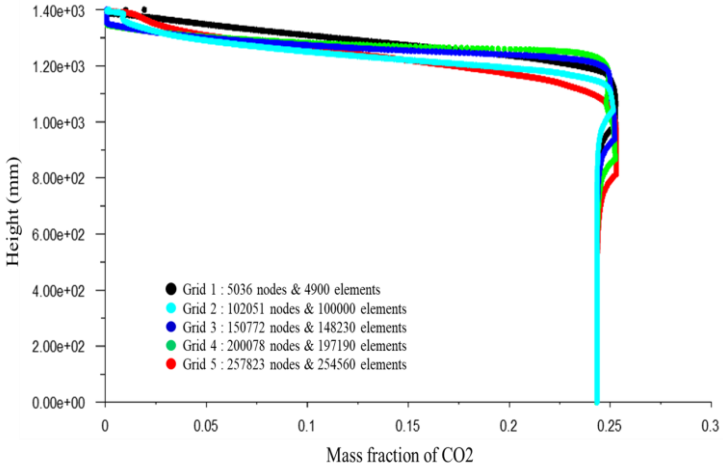

Fig. 3. Grid independence tests of mass fraction of CO2 in various grid.

The simulation results comparing combustion coal originating from Kalimantan demonstrate significant differences. Fig. 4 illustrates the variation in combustion temperature at the centerline DTF for simulation results with RP, KC, and MB. According to the simulation findings, the MB coal has the most consistent combustion temperature, maintaining a temperature of 900°C from a height of 200 mm to 1200 mm. RP coal shows the highest combustion temperature but fluctuates throughout the furnace. On the other hand, KC coal displays the lowest combustion temperature for a height of 400 mm to 1200 mm, with a temperature of 600°C. However, the temperature rises from 400 mm to the bottom, from 600°C to 1200°C.

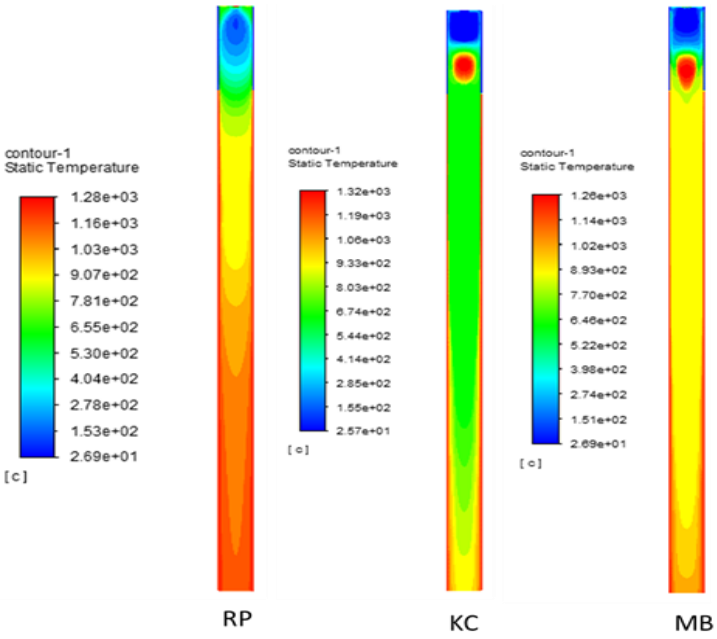

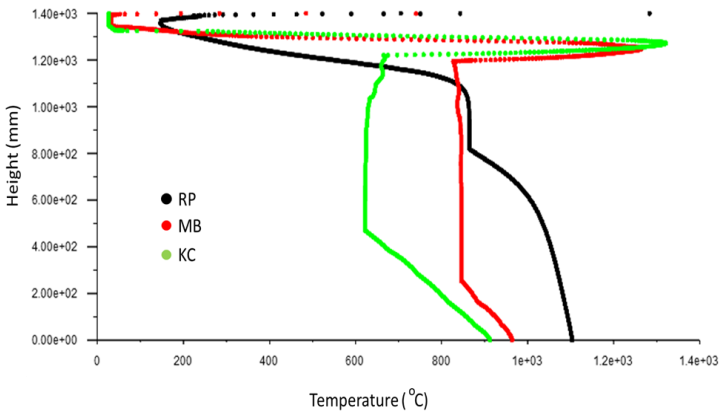

Fig. 4. Contour and Graph of comparison Temperature

Fig. 5 displays the contour and graph of the NOx pollutant in the centerline furnace. Once the fuel is introduced to the DTF (Drop tube furnace), it undergoes rapid combustion, resulting in a temporary elevation of the NOx mass fraction. Subsequently, the mass fraction of NOx stabilizes and remains constant. The results of the combustion simulation reveal no significant differences in NOx levels between RP, KC, and MB coal at 0.15 mass fraction. The highest level of NOX is observed when coal is added to meet hot air, followed by a gradual decrease until it remains constant at the height of 1300 mm. Fig. 5 shows that KC coal has the highest NOx pollutant level with 0.156 mass fraction NOx, while RP coal has the lowest with 0.14 mass fraction NOx.

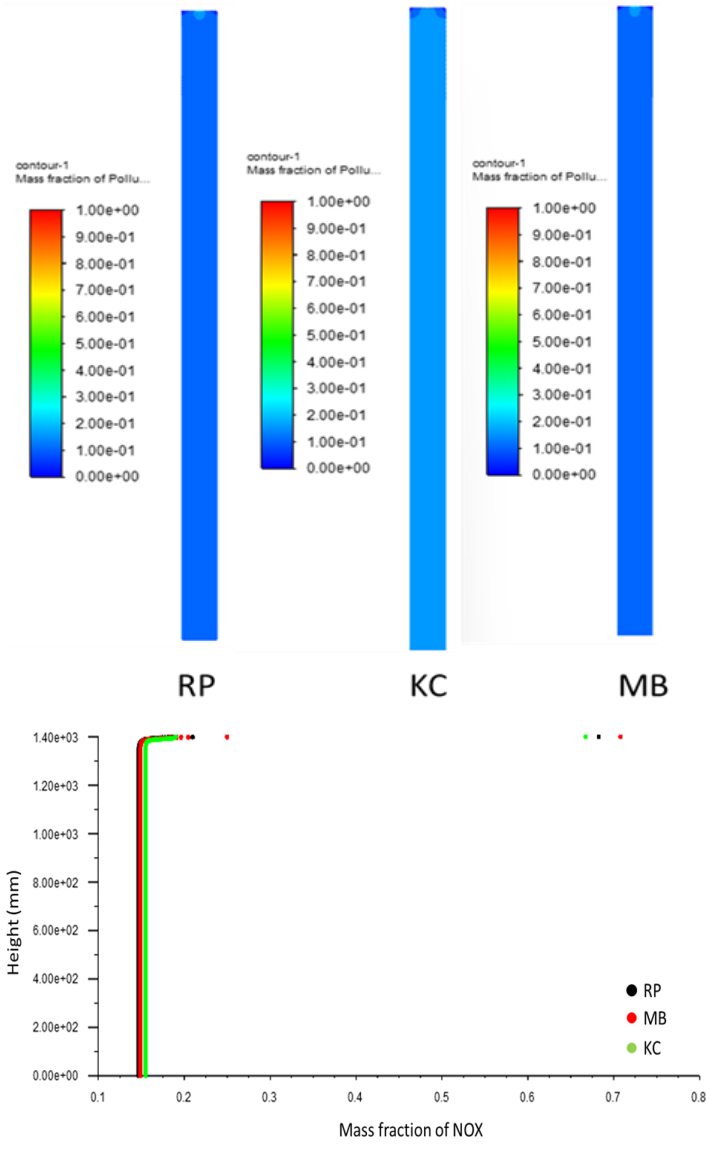

Fig. 5. Contour and Graph of comparison NOX

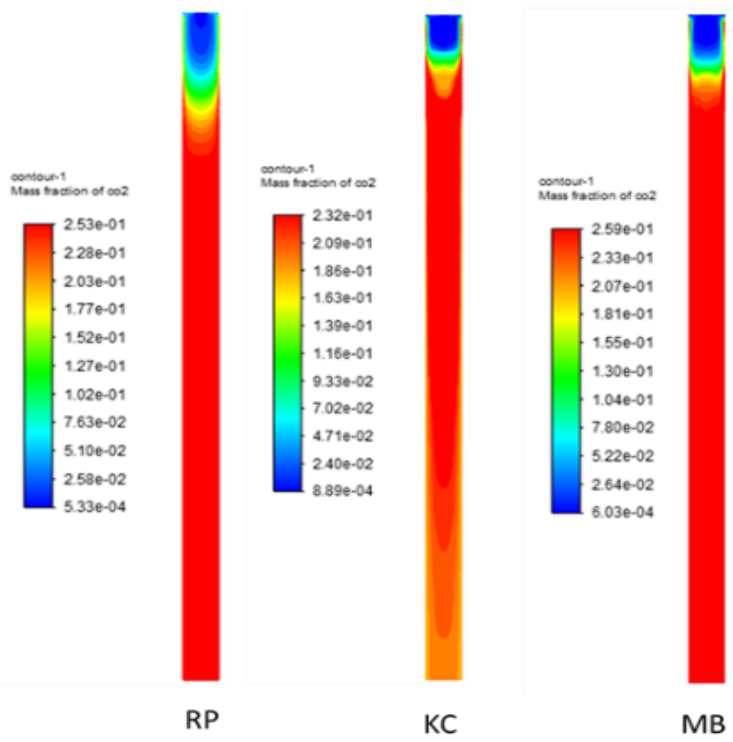

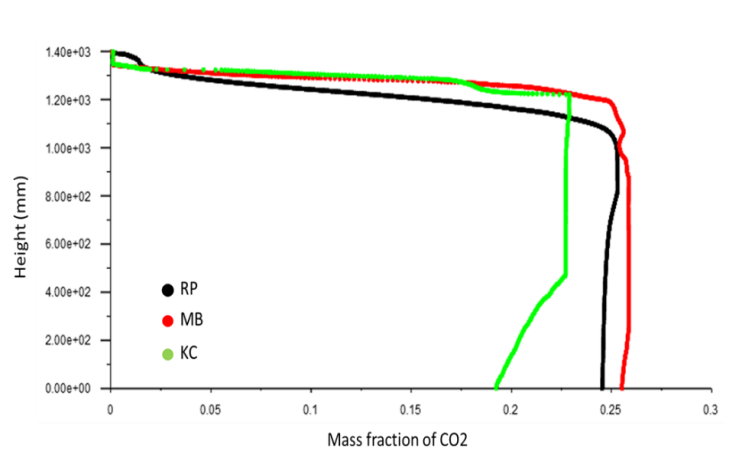

Fig. 6. Contour and Graph of comparison CO_2

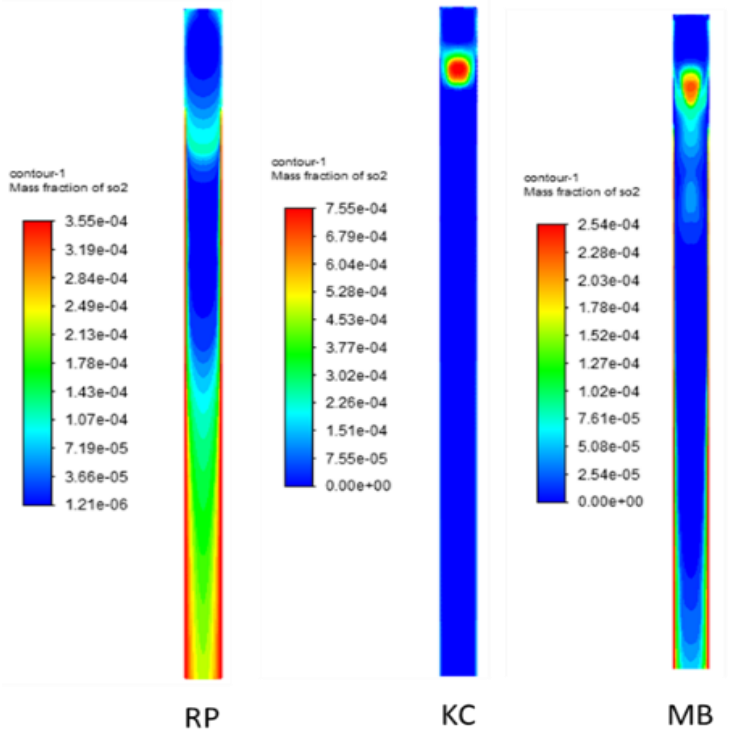

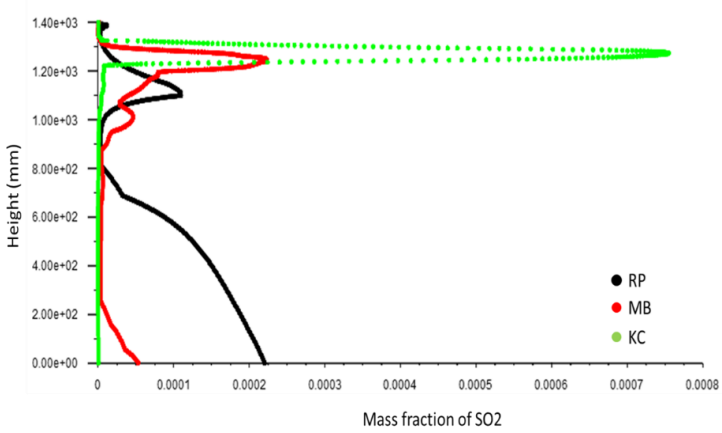

Fig. 7. Contour and Graph of comparison SO_2

Fig. 6 illustrates the variations in CO_2 levels represented by the contours and graphs along the centerline. Among the three types of coal, MB coal shows the highest CO_2 mass fraction, reaching 0.26 at some points. Conversely, KC coal exhibits the lowest CO_2 mass fraction, with values of 0.22 maintained from the height of 400 mm to 1200 mm but dropping to 0.18 from 400 mm to the bottom of the furnace. RP coal, on the other hand, maintains a relatively constant CO_2 mass fraction of 0.24 from 1000 mm to the bottom of the furnace.

Fig. 7 illustrates the contour and graph of SO_2, with the highest SO_2 mass fraction found in RP coal at 0.00022. In KC coal, there is a significant increase at the beginning of coal entry, which then decreases and remains constant. KC coal has the lowest SO_2 levels in this combustion simulation. The combustion simulation results for MB coal did not change significantly, with only 0.00005 mass fraction of SO_2.

3 Conclusions

The drop tube furnace (DTF) coal combustion simulation for evaluating the temperature and pollutants using a Non-premix combustion model and Probability Density Function (PDF) has been developed. Simulations of pulverized coal combustion have been carried out to measure and compare temperature, NOx, SO2, and CO2. Further studies are needed to axisymmetric assumptions and reduce pollutants by co-firing or oxy-fuel combustion.

Abbreviation:

DTF : Drop tube furnace
PDF : Probability Density Function
CFD : Computational fluid dynamics
RP : Coal from South Kalimantan
KC : Coal from East Kalimantan
MB : Coal from East Kalimantan

References

[1] B. K. Yun and M. Y. Kim, "Modeling the selective catalytic reduction of NOx by ammonia over a Vanadia-based catalyst from heavy duty diesel exhaust gases," *Appl. Therm. Eng.*, vol. 50, no. 1, pp. 152–158, 2013, doi: https://doi.org/10.1016/j.applthermaleng.2012.05.039.

[2] J. M. Gomes Antunes, R. Mikalsen, and A. P. Roskilly, "An investigation of hydrogen-fuelled HCCI engine performance and operation," *International Journal of Hydrogen Energy*, vol. 33, no. 20. pp. 5823–5828, 2008. doi: 10.1016/j.ijhydene.2008.07.121.

[3] K. Kang, S.-K. Hong, D.-S. Noh, and H.-S. Ryou, "Heat transfer characteristics of a ceramic honeycomb regenerator for an oxy-fuel combustion furnace," *Appl. Therm. Eng.*, vol. 70, no. 1, pp. 494–500, 2014, doi: https://doi.org/10.1016/j.applthermaleng.2014.05.053.

[4] V. Gogulancea and V. Lavric, "Flue gas cleaning by high energy electron beam – Modeling and sensitivity analysis," *Appl. Therm. Eng.*, vol. 70, no. 2, pp. 1253–1261, 2014, doi: https://doi.org/10.1016/j.applthermaleng.2014.05.046.

[5] J. Shen, J. Liu, H. Zhang, and X. Jiang, "NOx emission characteristics of superfine pulverized anthracite coal in air-staged combustion," *Energy Convers. Manag.*, vol. 74, pp. 454–461, 2013, doi: https://doi.org/10.1016/j.enconman.2013.06.048.

[6] I. E. Agency, "Global Energy Review : CO2 Emissions in 2021 Global emissions rebound sharply to highest ever level INTERNATIONAL ENERGY," 2021, [Online]. Available: https://www.iea.org/reports/global-energy-review-co2-emissions-in-2021-2

[7] M. of E. and M. R. R. of Indonesia, "Handbook Energy & Economic Statistics Indonesia," *Minist. Energy Miner. Resour. Repub. Indones.*, pp. 23–26, 2021, [Online]. Available: https://www.esdm.go.id/en/publication/handbook-of-energy-economic-statistics-of-indonesia-heesi

[8] D. T. Pratt, L. Smoot, and D. Pratt, *Pulverized coal combustion and gasification*. Springer, 1979. doi: https://doi.org/10.1007/978-1-4757-1696-2.

[9] V. Sahajwalla, A. Eghlimi, and K. Farrell, "Numerical simulation of pulverized coal combustion," *CSIRO Div. Miner. Melbourne, Vic.*, 1997, [Online]. Available: https://www.osti.gov/etdeweb/biblio/300871

[10] H. Ettouati, A. Boutoub, H. Benticha, and M. Sassi, "Radiative heat transfer in pulverized coal combustion: Effects of gas and particles distributions," *Turkish J. Eng. Environ. Sci.*, vol. 31, no. 6, pp. 345–353, 2007, [Online]. Available: https://www.researchgate.net/publication/237397379_Radiative_Heat_Transfer_in_Pulverized_Coal_Combustion_Effects_of_Gas_and_Particles_Distributions

[11] B. Rahmanian Kooshkaki and M. Ghazikhani, "Effect of steam injection in pulverized coal combustion to reduce pollutants," 2009. [Online]. Available: https://profdoc.um.ac.ir/paper-abstract-1013740.html

[12] B. Rahmanian, M. R. Safaei, S. N. Kazi, G. Ahmadi, H. F. Oztop, and K. Vafai, "Investigation of pollutant reduction by simulation of turbulent non-premixed pulverized coal combustion," *Appl. Therm. Eng.*, vol. 73, no. 1, pp. 1222–1235, 2014, doi: 10.1016/j.applthermaleng.2014.09.016.

[13] L. L. Dong, W. L. Zhao, and N. N. Xing, "Analysis of Pulverized Coal Combustion in Precalciner Based on Fluent Software," in *Advanced Design and Manufacturing Technology IV*, 2014, vol. 635, pp. 40–43. doi: 10.4028/www.scientific.net/AMM.635-637.40.

[14] M. P. K. Naik and S. K. Dewangan, "CFD modeling of non-premixed combustion of pulverized coal in a furnace," *Comput. Therm. Sci. An Int. J.*, 2017, doi: 10.1615/ComputThermalScien.2017019027.

[15] W. Sun, W. Zhong, and T. Echekki, "Large eddy simulation of non-premixed pulverized coal combustion in corner-fired furnace for various excess air ratios," *Appl. Math. Model.*, vol. 74, no. x, pp. 694–707, 2019, doi: 10.1016/j.apm.2019.05.017.

[16] S. K. Dewangan, M. P. K. Naik, and V. Deshmukh, "Parametric Study Of The Non-Premixed Coal Combustion In Furnace For Heat Transfer And Emission Characteristics," *J. Therm. Eng.*, vol. 6, no. 6, pp. 323–353, 2020, doi: 10.18186/THERMAL.833556.

[17] J. Han *et al.*, "Fine Ash Formation and Slagging Deposition during Combustion of Silicon-Rich Biomasses and Their Blends with a Low-Rank Coal," *Energy \& Fuels*, vol. 33, no. 7, pp. 5875–5882, 2019, doi: 10.1021/acs.energyfuels.8b04193.

[18] S. Hui, Y. Lv, Y. Niu, S. Li, Y. Lei, and P. Li, "Effects of leaching and additives on the formation of deposits on the heating surface during high-Na/Ca Zhundong coal combustion," *J. Energy Inst.*, vol. 94, pp. 319–328, 2021, doi: https://doi.org/10.1016/j.joei.2020.09.016.

[19] X. Li, X. Gong, C. Zhang, T. Liu, W. Wang, and Y. Zhang, "Occurrence characteristics of ash-forming elements in sea rice waste and their effects on particulate matter emission during combustion," *Fuel*, vol. 273, p. 117769, 2020, doi: https://doi.org/10.1016/j.fuel.2020.117769.

[20] Y. Yang *et al.*, "Investigation on the effects of different forms of sodium, chlorine and sulphur and various pretreatment methods on the deposition characteristics of Na species during pyrolysis of a Na-rich coal," *Fuel*, vol. 234, pp. 872–885, 2018, doi: https://doi.org/10.1016/j.fuel.2018.07.130.

[21] Hariana, F. Karuana, Prabowo, E. Hilmawan, A. Darmawan, and M. Aziz, "Effects of Different Coals for Co-Combustion with Palm Oil Waste on Slagging and Fouling Aspects," *Combust. Sci. Technol.*, vol. 00, no. 00, pp. 1–23, 2022, doi: 10.1080/00102202.2022.2152684.

[22] T. Echekki and E. Mastorakos, "Turbulent combustion: Concepts, governing equations and modeling strategies," *Fluid Mech. its Appl.*, vol. 95, pp. 19–39, 2011, doi: 10.1007/978-94-007-0412-1_2.

[23] Z. Q. Li, F. Wei, and Y. Jin, "Numerical simulation of pulverized coal combustion and NO formation," *Chem. Eng. Sci.*, vol. 58, no. 23, pp. 5161–5171, 2003, doi: https://doi.org/10.1016/j.ces.2003.08.012.

[24] M. R. Safaei, H. Goshayeshi, B. Razavi, and M. Goodarzi, "Numerical investigation of laminar and turbulent mixed convection in a shallow water-filled enclosure by various turbulence methods," vol. 6, 2010, [Online]. Available: https://www.researchgate.net/publication/267850752_Numerical_investigation_of_laminar_and_turbulent_mixed_convection_in_a_shallow_water-filled_enclosure_by_various_turbulence_methods

[25] M. Goodarzi *et al.*, "Numerical Study of Entropy Generation due to Coupled Laminar and Turbulent Mixed Convection and Thermal Radiation in an Enclosure Filled with a Semitransparent Medium," *Sci. World J.*, vol. 2014, p. 761745, 2014, doi: 10.1155/2014/761745.

[26] E. Sistani, *PIV measurements around a rotating single gear partially submerged in oil within modelled SAAB gearbox*. Citeseer, 2010. [Online]. Available: https://hdl.handle.net/20.500.12380/128553

[27] X. Cui, K. J. Chua, W. M. Yang, K. C. Ng, K. Thu, and V. T. Nguyen, "Studying the performance of an improved dew-point evaporative design for cooling application," *Appl. Therm. Eng.*, vol. 63, no. 2, pp. 624–633, 2014, doi: https://doi.org/10.1016/j.applthermaleng.2013.11.070.

[28] M. A. Habib, R. Ben-Mansour, H. M. Badr, S. A. M. Said, and S. S. Al-Anizi, "Erosion in the tube entrance region of a shell and tube heat exchanger," *Int. J. Numer. Methods*

Heat Fluid Flow, vol. 15, no. 2, pp. 143–160, Jan. 2005, doi: 10.1108/09615530510578429.

[29] M. A. Habib, H. M. Badr, S. A. M. Said, R. Ben-Mansour, and S. S. Al-Anizi, "Solid-particle erosion in the tube end of the tube sheet of a shell-and-tube heat exchanger," *Int. J. Numer. Methods Fluids*, vol. 50, no. 8, pp. 885–909, 2006, doi: https://doi.org/10.1002/fld.1083.

[30] B. Yan, Y. Cheng, Y. Jin, and C. Y. Guo, "Analysis of particle heating and devolatilization during rapid coal pyrolysis in a thermal plasma reactor," *Fuel Process. Technol.*, vol. 100, pp. 1–10, 2012, doi: https://doi.org/10.1016/j.fuproc.2012.02.009.

[31] I. Glassman and R. A. Yetter, "Chapter 8 - Environmental Combustion Considerations," in *Combustion (Fourth Edition)*, Fourth Edi., I. Glassman and R. A. Yetter, Eds. Burlington: Academic Press, 2008, pp. 409–494. doi: https://doi.org/10.1016/B978-0-12-088573-2.00008-7.

[32] ANSYS, "ANSYS FLUENT 12.0/12.1 Documentation," *Fluent manual book*, 2012. https://www.afs.enea.it/project/neptunius/docs/fluent/html/th/node212.htm

[33] M. R. Safaei, B. Rahmanian, and M. Goodarzi, "Numerical study of laminar mixed convection heat transfer of power-law non-Newtonian fluids in square enclosures by finite volume method," vol. 6, 2010, doi: 10.5897/ijps11.1092.

[34] M. Goodarzi *et al.*, "Investigation of nanofluid mixed convection in a shallow cavity using a two-phase mixture model," *Int. J. Therm. Sci.*, vol. 75, pp. 204–220, 2014, doi: https://doi.org/10.1016/j.ijthermalsci.2013.08.003.